

*J.Serb.Chem.Soc.* 66(11–12)811–823(2001)  
*JSCS* –2905

UDC 531.3:546.11+541.18+546.47:549.3  
*Original scientific paper*

## On the kinetics of the hydrogen evolution reaction on zinc in sulfate solutions\*

T. TRIŠOVIĆ<sup>1</sup>, L.J. GAJIĆ-KRSTAJIĆ<sup>1</sup>, N. KRSTAJIĆ<sup>2#</sup> and M. VOJNOVIĆ<sup>2#</sup>

<sup>1</sup>*Institute of Technical Science, SASA, Kneza Mihajla 35, YU-11000 Belgrade and* <sup>2</sup>*Department of Physical Chemistry and Electrochemistry, Faculty of Technology and Metallurgy, University of Belgrade, Karnegijeva 4. YU-11000 Belgrade, Yugoslavia*

(Received 12 July, revised 29 August 2001)

The kinetics and mechanism of the hydrogen evolution reaction (her) were studied on zinc in 1.0 mol dm<sup>-3</sup> Na<sub>2</sub>SO<sub>4</sub> at 298 K, in the pH range 4.4 – 10. It was found that a combination of classical potentiostatic steady-state voltammetry (PSV) and electrochemical impedance spectroscopy (EIS) can help to elucidate dilemmas concerning the mechanism of this reaction. Thus, over the whole potential region, the reaction path of the her on zinc cannot be presented by the classical Volmer -Tafel-Heyrovsky route. It was found that the very complex S-shape of the polarization curves could be explained by two parallel reaction mechanisms for the her. The first reaction mechanism is a consecutive combination of three steps, in which the surface zinc oxide plays an active role in the her, and second reaction mechanism is a consecutive combination of a Volmer step, followed by a Heyrovsky step. The second mechanism is dominant in the more negative potential region where the active sites for the her are metallic zinc.

*Keywords:* hydrogen evolution reaction, zinc electrode, sulfate solution, spectroscopy of electrochemical impedance, mechanism, NLS fitting, rate constants.

### INTRODUCTION

The hydrogen evolution reaction (her) is one of the most frequently studied electrochemical reactions because it takes place through a limited number of reaction steps with the involvement of only one reaction intermediate. The reaction path of the her is classically based on (1) a discharge reaction (Volmer step) followed by either (2) a recombination reaction (Tafel step) and/or (3) an electrochemical desorption reaction (Heyrovsky step). Apart from the above mentioned reaction paths, steps different from (1) to (3) have rarely been suggested. Although the formation of Na<sub>ads</sub> on the electrode is probably well established on soft metals,<sup>1–3</sup> there still remains the discussion as to whether the Na<sub>ads</sub> is actually a reaction intermediate of the her or simply a by-product.

\* Dedicated to Professor Dragutin M. Dražić on the occasion of his 70th birthday.

# Serbian Chemical Society active member.

Other reaction routes involving reaction intermediates such as  $\text{H}_{2(\text{ads})}^+$ ,  $\text{H}_{\text{ads}}^-$ , and solvated electrons<sup>4,5</sup> have not gained sufficient experimental support to demonstrate that these species should be considered seriously which emphasizes the simplicity usually envisaged in the her. It is interesting to note that a new mechanism has been proposed for the her to account for the role played by surface oxides<sup>6</sup> possibly present in the potential region of the her. Drazic *et al.* proposed a mechanism for the her at Al electrode in the pH range 5–8 in which  $\text{H}_2$  evolves by the discharge of  $\text{H}_3\text{O}^+$  ions formed by the dissociation of water, which acts as the rate-determining step.<sup>7</sup>

The determination of the coverage by the reaction intermediate  $\text{H}_{\text{ads}}$  vs. the negative potential is another important feature of the kinetics of the her required for a better understanding of the mechanism. In recent years, considerable progress has been made in studies of adsorbed surface species at appreciable current densities by open-circuit potential decay (OPD)<sup>8–10</sup> and electrochemical impedance spectroscopy (EIS) methods.<sup>11–17</sup>

Extensive kinetic studies of the her by impedance spectroscopy have introduced new numerical simulation techniques of the observed complex-plane diagrams, which have opened up the possibilities of the evaluation of the rate constants for all steps, as discussed,<sup>18</sup> on the basis of fundamental analysis done by Armstrong and Henderson.<sup>19</sup>

The her on pure zinc has been investigated mainly in acid solutions because of its relevance to corrosion problems.<sup>20–22</sup> It has been noticed that the reproducibility is poor but at a fresh electrode surface the Tafel slope is usually around  $-0.12\text{ V}$ ,<sup>23–25</sup> pointing to the primary discharge being the rate determining step.

The her on zinc in neutral solutions has scarcely been investigated, and there is still no common agreement on the mechanism. Therefore, further investigations of the her are needed. We found a combination of classical potentiostatic steady-state voltammetry (PSV) and electrochemical impedance spectroscopy (EIS) to be a source of valuable experimental information on the kinetics of the her which can help to elucidate dilemmas concerning the mechanism of this reaction at zinc in neutral solutions.

## EXPERIMENTAL

*Cell and chemicals.* A conventional three-compartment cell was used. The working zinc electrode (WE) compartment was separated by fritted glass discs from the other two compartments. The WE compartment was jacketed and thermostated at  $25.0\text{ }^\circ\text{C}$  during the measurements.

All measurements were performed in  $1.0\text{ mol dm}^{-3}$  solution of  $\text{Na}_2\text{SO}_4$  (Spectrograde, Merck), prepared in deionized water. The pH of the solution was adjusted between 4.4 and 10.0 by addition of adequate amounts of phthalate buffer.

The WE compartment was saturated with purified hydrogen at standard pressure during the measurements.

*Electrodes.* Polycrystalline zinc wire (diam. 1 mm, purity 99.99 %) of  $1\text{ cm}^2$  exposed surface area was used as the WE. The counter electrode was a platinum sheet of  $5\text{ cm}^2$  geometric area. The reference electrode was saturated calomel electrode (SCE), held at a constant temperature of  $25.0\text{ }^\circ\text{C}$ . All values of the potential in this article are referred to the SCE.

*Pretreatment of the WE.* Before measurements, the WE was held for 10 min at  $-1.80\text{ V}$ . Steady-state measurements following ascending changes of the potential were performed. No significant hysteresis on the polarization curve was observed.

*Measurements.* Tafel lines were recorded using potentiostatic steady-state voltammetry, point by point at 60 s intervals, in the range of potential from  $-1.80$  to  $-1.05$  V, using a PAR 273 potentiostat. The reproducibility of the measurements was good.

The IR drop was systematically determined in all measurements using AC impedance methods. All the data presented in this article are corrected for the IR drop.

Simultaneously with the Tafel lines, electrochemical impedance spectra of the WE at selected constant potentials were determined, using a PAR 273 potentiostat, together with a PAR 5301 lock-in-amplifier, controlled through a GPBI PC2A interface. The fast Fourier transformation (FFT) technique was used to obtain the real ( $Z'$ ) and imaginary ( $Z''$ ) components of the WE impedance at each frequency used. So, impedance spectra in the complex plane diagrams were obtained in the frequency range from 50 mHz to 100 kHz. In all measurements above 5 Hz, ten frequency points per decade were taken.

#### RESULTS AND DISCUSSION

Typical polarization curves for the her in the extended region of potential, *i.e.*, from approximately  $-1.10$  to  $-1.80$  V, for different pH values (4.4–10.0) are presented in Fig. 1. The curves show typical limiting current behavior at  $\text{pH} \leq 8.0$  and for even more negative polarizations all the curves merge into a linear Tafel line with a slope of about  $-0.14$  V/dec.

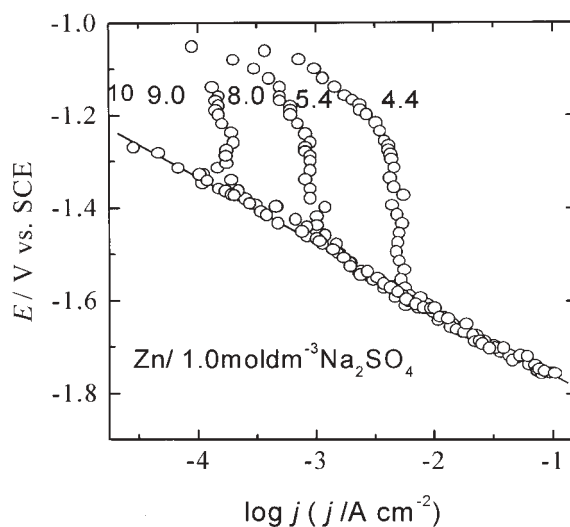


Fig. 1. Tafel polarization curves for the her on a Zn electrode in  $1.0 \text{ mol dm}^{-3} \text{ Na}_2\text{SO}_4$  solutions of different pH values at  $25.0 \text{ }^\circ\text{C}$ .

The electrochemical impedance spectra in the complex plane recorded at potentials where the limiting current had appeared, as presented in Fig. 2 for  $E = -1.297$  V, clearly indicate a charge transfer controlled process at the WE. Hence, any speculations on the nature of this curvilinear part of the polarization curve, such as a limiting current of various Faradaic processes different from the her, are strongly suspect.

Eight values of electrode potentials were selected to cover the entire polarization curve and impedance spectra of the WE in the complex plane were determined and are

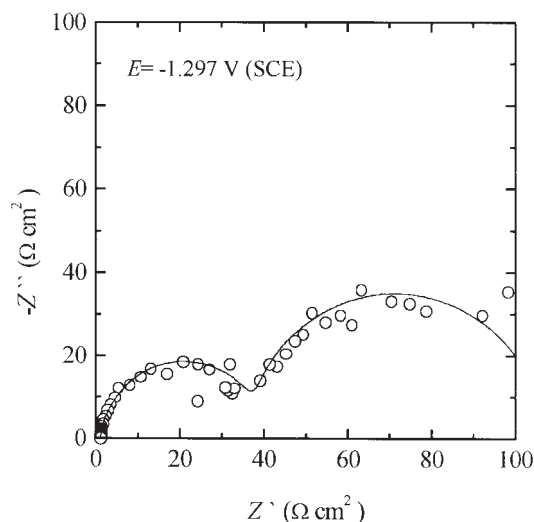


Fig. 2. Impedance spectrum in the complex plane for the her on Zn in 1.0 mol dm<sup>-3</sup> Na<sub>2</sub>SO<sub>4</sub> (pH 4.4) at 25.0 °C and at  $E = -1.297$  V, within the curvilinear part of the polarization curve in Fig. 1.

presented in Figs. 3 and 4. The circled points in Figs. 3 and 4 are experimental data and the lines were obtained by the NLS fitting procedure.

TABLE I. Calculated parameters of the modified Armstrong equivalent circuit (Fig. 5b) obtained by the NLS fitting procedure for the her on Zn in 1.0 mol dm<sup>-3</sup> Na<sub>2</sub>SO<sub>4</sub>, at pH 4.4 ( $R_{\Omega} = 1.08 \Omega \text{ cm}^2$ ).

$E/V$ (SCE)	$R_{ct}/\Omega \text{ cm}^2$	$R_{p1}/\Omega \text{ cm}^2$	$R_{p2}/\Omega \text{ cm}^2$	$C_{dl}/\mu\text{F cm}^{-2}$	$C_{p1}/\mu\text{F cm}^{-2}$	$C_{p2}/\mu\text{F cm}^{-2}$
-1.247	22.3	12.1	47.2	70.8	66.5	7117
-1.297	21.3	16.9	67.2	70.3	65.9	3341
-1.346	38	23.2	35.8	86.6	56	2393
-1.396	14.6	15.7	21.8	101.4	55.9	1131

TABLE II. Calculated parameters of the Armstrong equivalent circuit (Fig. 5a) obtained by the NLS fitting procedure for the her on Zn in 1.0 mol dm<sup>-3</sup> Na<sub>2</sub>SO<sub>4</sub>, at pH 4.4 ( $R_{\Omega} = 1.08 \Omega \text{ cm}^2$ ).

$E / V$ (SCE)	-1.54	-1.59	-1.63	-1.67
$R_{ct}/\Omega \text{ cm}^2$	19.5	11.9	7.8	5.5
$C_{dl}/\mu\text{F cm}^{-2}$	136	111	170	192

The impedance data obtained in the Tafel region (Fig. 4) were interpreted using the equivalent electric circuit of Armstrong and Henderson,<sup>19</sup> given in Fig. 5a, where  $R_{ct}$  is the charge transfer resistance for the electrode reaction at the WE,  $C_{dl}$  the double layer capacitance of the WE,  $R_p$  is basically related to the mass transfer resistance of the adsorbed intermediate  $H_{ads}$ , usually called the pseudo resistance, and  $C_p$  is the pseudo capacitance of the WE. The impedance data (Fig. 3) obtained in the curvilinear part of

the polarization curves were interpreted using a modified Armstrong electric circuit for an electrode reaction with two intermediate species (Fig. 5b), where  $R_{p1}$  and  $R_{p2}$  are pseudo resistancies related to the dependence of the electrode reaction rate on the coverage of the adsorbed intermediates at constant potential, and  $C_{p1}$  and  $C_{p2}$  are the pseudo capacitances of the WE.

The data presented in Figs. 3 and 4 were interpreted by NLS fitting procedure<sup>26</sup> to determine the elements of the Armstrong equivalent circuit of the WE, given in Fig. 5. The values of all parameters obtained by this procedure are presented in Tables I and II. The values of the parameters in Tables I and II were then used to interpret the kinetics of the her.

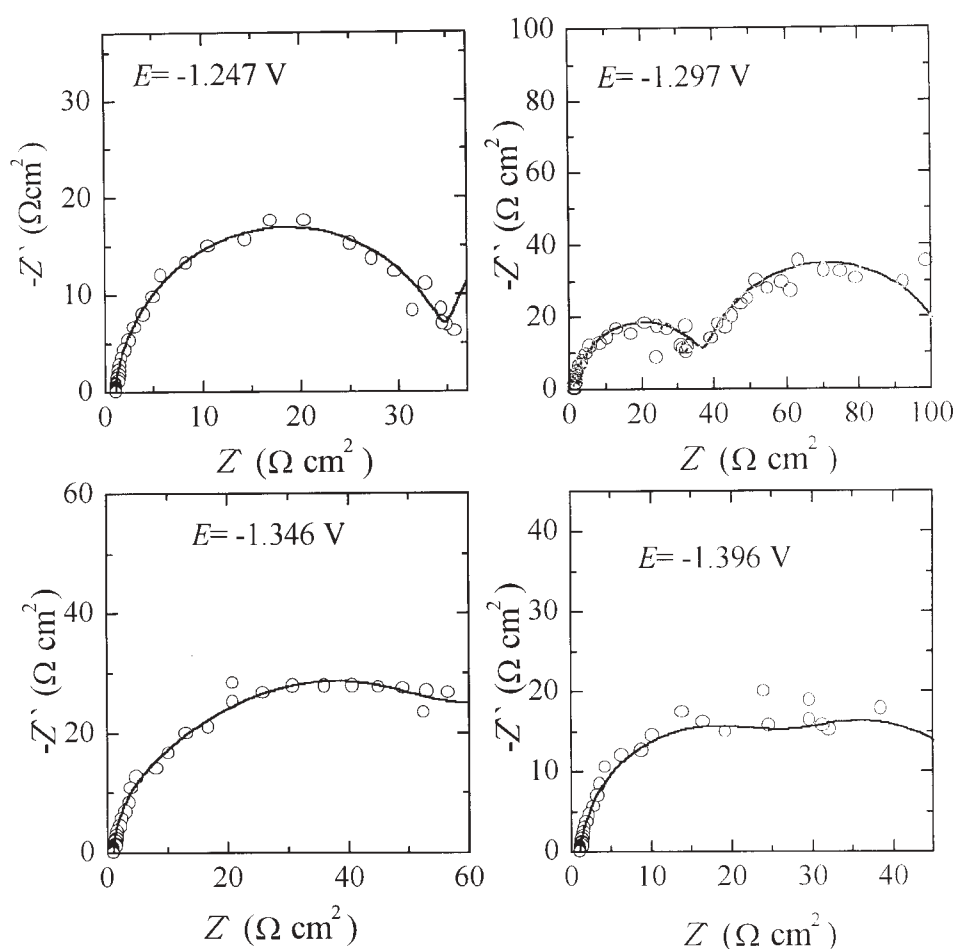


Fig. 3. Impedance spectra in the complex plane for the her on Zn in  $1.0 \text{ mol dm}^{-3} \text{ Na}_2\text{SO}_4$  (pH 4.4) at  $25.0 \text{ }^\circ\text{C}$ , at four constant potentials indicated within curvilinear part of the polarization curve in Fig. 1. The circles are experimental points and the solid lines are calculated using the NLS fitting procedure.

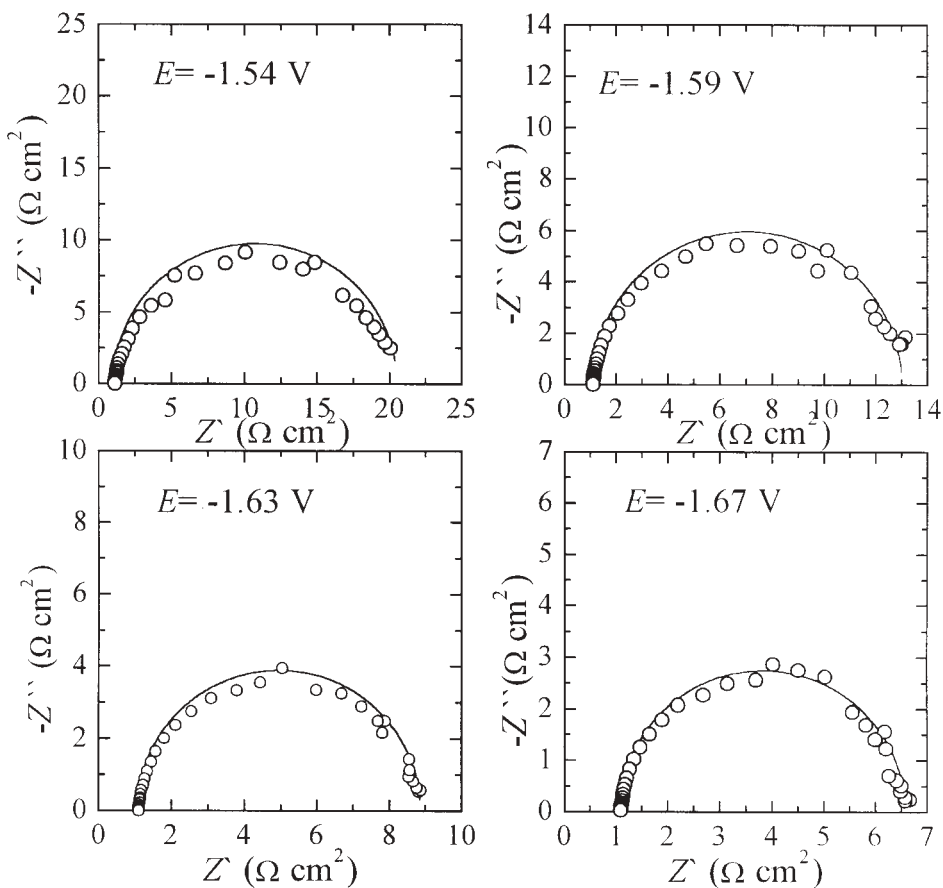


Fig. 4. Impedance spectra in the complex plane for the her on Zn in  $1.0 \text{ mol dm}^{-3} \text{ Na}_2\text{SO}_4$  (pH 4.4) at  $25.0^\circ\text{C}$ , at four constant potentials indicated within Tafel region of the polarization curve in Fig. 1. The circles are experimental points and the solid lines are calculated using the NLS fitting procedure.

#### *Analysis of the PSV data*

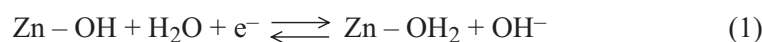
*Curvilinear part of the polarization curve.* In the analysis of the curvilinear part of the polarization curves for the her on Zn it is important to emphasize the following facts:

- a) The value of the limiting current is much higher than the corresponding diffusion current for the reduction of  $\text{H}_3\text{O}^+$  ions at a certain pH value of the solution and does not vary with the rotation speed of the WE,
- b) The limiting current does not vary with holding time of the potential, which excludes the possibility that the reduction of surface oxides or corrosion products takes place in this potential range,

c) The shape of the impedance spectrum taken at the potential of limiting current clearly indicates that the reaction is under charge transfer control, and finally,

d) It is possible to obtain limiting current behavior of the polarization curve for the her when a Volmer-Tafel route is operative in which a recombination step (Tafel step) is rate controlling, but it is not possible in this case to re-establish the Tafel region at more negative potentials, as was the case with the obtained experimental polarization curves.

Generally, the limiting current behavior of the polarization curves for the her on Zn could be explained by a mechanism in which surface oxide plays<sup>5</sup> an active role. The proposed mechanism consists of two electrochemical and one chemical step:



The corresponding theoretical rate of each step where the surface concentration of the intermediates Zn-OH<sub>2</sub> and Zn-H, and corresponding free adsorption sites at the WE are given as coverages, or surface concentration fractions,  $\theta_{\text{O}}$ ,  $\theta_{\text{H}}$  and  $1-(\theta_{\text{O}} + \theta_{\text{H}})$  are respectively:

$$v_1 = k_1(1-\theta_{\text{O}} - \theta_{\text{H}})\exp\left(\frac{\beta_1 F}{RT} \eta\right) - k_{-1}\theta_{\text{O}} \exp\left[\frac{-(1-\beta_1)F}{RT} \eta\right]$$

$$v_1 = k_1'(1-\theta_{\text{O}} - \theta_{\text{H}}) - k_{-1}'\theta_{\text{O}} \quad (4)$$

$$v_2 = k_2\theta_{\text{O}} \exp\left(\frac{\beta_2 F}{RT} \eta\right) - k_{-2}\theta_{\text{H}} \exp\left[\frac{-(1-\beta_2)F}{RT} \eta\right]$$

$$v_2 = k_2' - k_{-2}'\theta_{\text{H}} \quad (5)$$

$$v_3 = k_3\theta_{\text{H}} - k_{-3}(1-\theta_{\text{H}} - \theta_{\text{O}}) \quad (6)$$

where  $k_i$  and  $k_{-i}$  are the chemical rate constants of the forward and backward reactions, respectively, for the  $i$ th step. They include the concentration of OH<sup>-</sup>, H<sub>2</sub>O and the H<sub>2</sub> pressure and are in the same units as  $v_1$  (mol cm<sup>-2</sup> s<sup>-1</sup>).

The total current density is

$$j = F(v_1 + v_2) \quad (7)$$

Under steady state conditions, the rates of the consecutive steps are equal, which means that rate of electrochemical adsorption and desorption steps of H<sub>ads</sub> are equal, *i.e.*,  $v_2 = v_3$

$$k_2'\theta_{\text{O}} - k_{-2}'\theta_{\text{H}} = k_3\theta_{\text{H}} - k_{-3}(1 - \theta_{\text{H}} - \theta_{\text{O}}) \quad (8)$$

Assuming that the backward reaction (3) can be neglected, it is possible to obtain the relationships between the coverage of the adsorbed intermediate species,  $\theta_{\text{O}}$  and  $\theta_{\text{H}}$ :

$$\theta_{\text{O}} = \theta_{\text{H}} \frac{k_3 + k_{-2}'}{k_2'}, \quad \theta_{\text{H}} = \theta_{\text{O}} \frac{k_2'}{k_3 + k_{-2}'} \quad (9)$$

At more negative potentials, the backward reaction of the second step can also be neglected, *i.e.*,  $k_{-2} \rightarrow 0$ , and Eq. (9) simplifies to:

$$\theta_{\text{O}} = \theta_{\text{H}} \frac{k_3}{k_2'} \quad \text{and} \quad \theta_{\text{H}} = \theta_{\text{O}} \frac{k_2'}{k_3} \quad (10)$$

Under steady state conditions, the rate of the first step is equal to the rate of the second elementary step, *i.e.*,  $v_1 = v_2$ :

$$k_1'(1 - \theta_{\text{H}} - \theta_{\text{O}}) - k_{-1}'\theta_{\text{O}} = k_2'\theta_{\text{O}} - k_{-2}'\theta_{\text{H}} \quad (11)$$

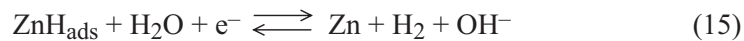
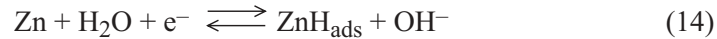
Combining Eqs. (10) and (11), it is possible to obtain the equations for the dependence of the coverage of the corresponding intermediate species on the overpotential:

$$\theta_{\text{H}} = \frac{k_1' k_2'}{k_1' k_2' + k_3' (k_1' + k_{-1}' + k_2')} \quad (12)$$

$$\theta_{\text{O}} = \frac{k_1' k_3}{k_1' k_2' + k_3' (k_1' + k_{-1}' + k_2')} \quad (13)$$

Equations (12) and (13) enable the surface coverage of adsorbed intermediate species and the rate of steps (1), (2) and (3) to be calculated in dependence on the overpotential, if the corresponding rate constants,  $k_i'$  are known. However, it is not possible to calculate with great accuracy the rate constants by the NLS fitting procedure of the PSV data. Hence, the rate constants were calculated by the NLS fitting procedure of the SEI data.

*Tafel region of the polarization curves.* As was stated earlier, all the polarization curves for the her at Zn obtained at different pH values merge into a unique Tafel line at more negative potentials, with a slope of  $-0.14$  V/dec. In this case it is reasonable to assume that the her takes place at metallic Zn sites through parallel Volmer-Heyrovsky route<sup>3</sup> as the dominant route at more negative potentials



The reaction rates of the two steps are given by

$$v_{\text{V}} = k_{\text{V}}(1 - \theta_{\text{H}}) \exp\left(-\frac{\beta F \eta}{RT}\right) - k_{-\text{V}} \theta_{\text{H}} \left[ \frac{(1 - \beta) F \eta}{RT} \right]$$

$$v_{\text{V}} = k'_{\text{V}}(1 - \theta_{\text{H}}) - k_{-\text{V}}' \theta_{\text{H}} \quad (16)$$



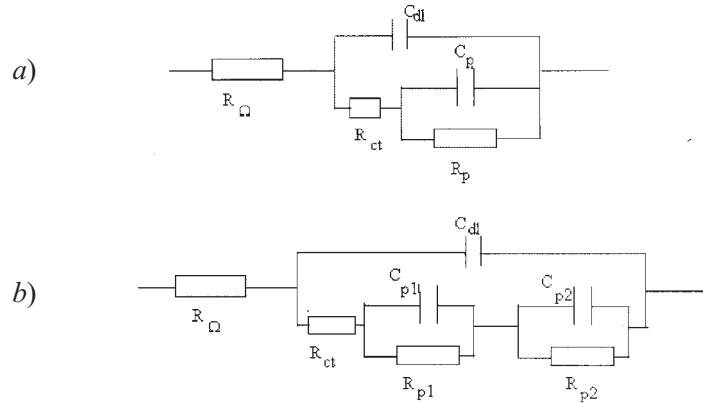


Fig. 5. a) The Armstrong equivalent electric circuit of the WE and b) A modified Armstrong equivalent electric circuit of the WE.  $R_{\Omega}$  is the ohmic resistance (uncompensated resistance) of the solution,  $R_{ct}$  is the charge transfer resistance,  $C_{dl}$ , the double layer capacitance,  $R_{pi}$ , the pseudo resistance and  $C_{pi}$ , the pseudo capacitance.

$$v_H = k_H \theta_H \exp\left(-\frac{\beta F \eta}{RT}\right) - k_{-H} (1 - \theta_H) \exp\left[\frac{(1 - \beta) F \eta}{RT}\right]$$

$$v_H = k_H' \theta_H - k_{-H}' (1 - \theta_H) \tag{17}$$

where  $k_i'$  ( $i = \pm V, \pm H$ ) are the potential dependent rate constants for the Volmer and the Heyrovsky steps.

The charge balance ( $r_0$ ) under a constant current density ( $j$ ), and the mass balance ( $r_1$ ) of the fractional surface coverage ( $\theta_H$ ) are given by the following equations:

$$r_0 = j / F = -2 (v_V + v_H) \tag{18}$$

$$r_1 = (q / F) (\partial \theta / \partial t) = v_V - v_H \tag{19}$$

where  $j$  is the current density for the her and  $q$  is the maximum surface charge corresponding to a surface  $\theta_H$  equal to 1.

The steady-state H coverage,  $\theta$ , is given by setting  $r_1 = 0$ , then:

$$\theta_H = \frac{k_V' + k_{-H}'}{k_V + k_{-V}' + k_H' + k_{-H}'} \tag{20}$$

Equation (20) also enables the surface coverage of adsorbed intermediate species and the reaction rate of steps (16) and (17) to be calculated in dependence of the overpotential, if the corresponding rate constants,  $k_i'$  are known.

At the equilibrium condition ( $v_V = v_H = 0$ ), the relationship between the  $k_i$  values can be represented by:

$$k_{-H} = \frac{k_V k_H}{k_{-V}} \quad (21)$$

Equation (21) allows the number of independent parameters in the  $k_i$  values to be reduced from four to three.

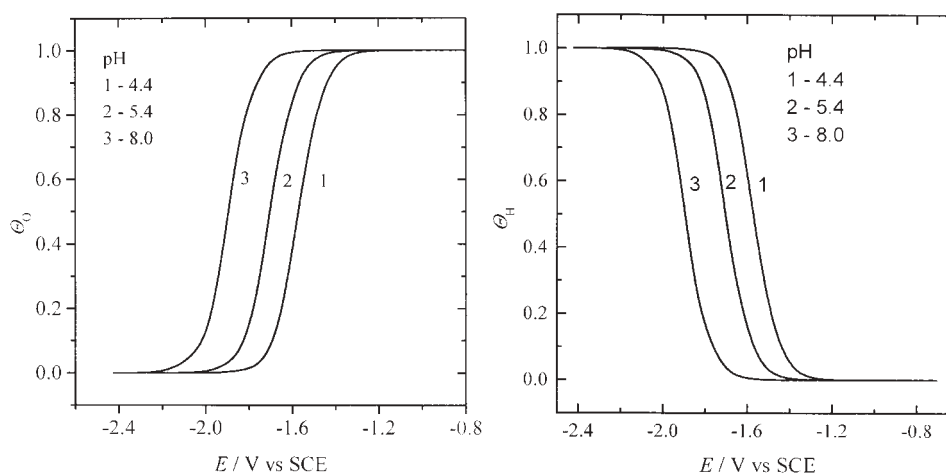


Fig. 6. Potential dependence of the calculated surface coverages by adsorbed intermediates a)  $\theta_O$  and b)  $\theta_H$  at a Zn electrode in  $1.0 \text{ mol dm}^{-3} \text{ Na}_2\text{SO}_4$  solutions of different pH values at  $25.0^\circ \text{C}$  (first reaction route).

#### Analysis of SEI data

*The curvilinear part of the polarization curves.* Theoretically, six variables, *i.e.*, four independent chemical rate constants,  $k_i$  ( $i = \pm 1, \pm 2$ ) of the three consecutive steps in the first reaction route (steps (1)–(3)) and two symmetry factors of the electrochemical steps ( $\beta_1$  and  $\beta_2$ ), describe the mechanism of the her at Zn in the curvilinear part of the polarization curves. However, it can be reasonably assumed for elementary electrode reactions that  $\beta_1 = \beta_2 = 0.5$ . With this assumption the problem is reduced to four independent variables. Hence, to calculate the values of the chemical rate constants for the basic steps of the her, four independent equations which describe their kinetics at the WE are required.

The method of factorial fitting and minimizing residuals (S) of the sum of each experimental datum (either PSV or EIS) was used, in accordance with a procedure described earlier<sup>26</sup> to calculate the corresponding values of the chemical rate constants,  $k_i$ .

The corresponding values of the chemical rate constants were calculated and are presented in Table III.

Using the values of the rate constants from Table III and Eqs. (12) and (13) it is possible to calculate the dependence of  $\theta_O$  and  $\theta_H$  on the potential of the WE. These dependencies are presented in Figs. 6a. and 6b. At potentials close to  $E_c(\text{her})$ , the calcu-

lated values of  $\theta_H$  are rather low, and the Zn electrode is almost fully covered by the Zn–OH<sub>2</sub> intermediate. At limiting current potentials,  $\theta_O$  decreases sharply while  $\theta_H$  increases and the zinc electrode is almost fully covered by H<sub>ads</sub>. It is interesting that the theoretically calculated value of the maximum charge of the WE (*i.e.*, corresponding to  $\theta_H \rightarrow 1$ ), obtained in the above mentioned procedure of fitting the experimental data, is close to 80  $\mu\text{C cm}^{-2}$  (pH 4.4), which is approximately one third of the hypothetical charge required to cover each surface atom of zinc by H<sub>ads</sub>, which was calculated for the (111) plane of Zn<sup>27</sup> to be 250  $\mu\text{C cm}^{-2}$ . Hence, in 1.0 mol dm<sup>-3</sup> Na<sub>2</sub>SO<sub>4</sub> at pH 4.4, the number of sites at the surface of the zinc electrode covered by the oxide is approximately one third of the total sites.

*Tafel region of the polarization curves.* For the second reaction route, the  $\theta_H$  vs.  $\eta$  relationship was calculated using the corresponding values of the rate constants from Table III and Eq. (20). The coverage of the electrode by H<sub>ads</sub> reaches an almost constant value of  $\theta_H = 0.03$  in Tafel region. The very low coverage by H<sub>ads</sub> and the Tafel slope of  $-0.14$  V/dec unambiguously indicates that a Volmer step is rate controlling in the Volmer-Heyrovsky reaction route which is the dominant mechanism at more negative potentials, where the her takes place at metallic zinc.

TABLE III. Calculated values of the chemical rate constants for the individual steps of the her on Zn in 1.0 mol dm<sup>-3</sup> Na<sub>2</sub>SO<sub>4</sub> solutions of different pH values.

k / mol cm <sup>-2</sup> s <sup>-1</sup>										
First reaction route					Second reaction route					
pH	$k_1$	$k_{-1}$	$k_2$	$k_{-2}$	$k_3$	$k_{-3}$	$k_V$	$k_{-V}$	$k_H$	$k_{-H}$
4.4	$5.5 \times 10^{-14}$	$1 \times 10^{-15}$	$3.0 \times 10^{-18}$	$1 \times 10^{-14}$	$2.5 \times 10^{-8}$	–	$2.7 \times 10^{-22}$	–	$8.0 \times 10^{-21}$	–
5.4	$5.5 \times 10^{-14}$	$1 \times 10^{-15}$	$1.2 \times 10^{-18}$	$1 \times 10^{-14}$	$5.0 \times 10^{-9}$	–	$2.7 \times 10^{-22}$	–	$8.0 \times 10^{-21}$	–
8.0	$5.5 \times 10^{-14}$	$1 \times 10^{-15}$	$8.0 \times 10^{-19}$	$1 \times 10^{-14}$	$8.5 \times 10^{-10}$	–	$2.7 \times 10^{-22}$	–	$8.0 \times 10^{-21}$	–
10.0	–	–	–	–	–	–	$2.7 \times 10^{-22}$	–	$8.0 \times 10^{-21}$	–

### Mechanism of the her

On the base of all the experimental and calculated data the following information concerning the kinetics of the her at zinc in 1.0 mol cm<sup>-3</sup> Na<sub>2</sub>SO<sub>4</sub> at 25 °C and for different pH values of the solution, can be summarized:

– Generally, the her occurs *via* two parallel mechanisms. The first mechanism is considered to be the consecutive combination of three steps with the heterogeneous chemical step as the rate controlling one. This mechanism is dominant in the potential range from the open circuit potential (OCP) up to the potentials where limiting current appears. The active sites for the her in the proposed mechanism are surface zinc oxide. The limiting current is a heterogeneous reaction limiting current which appears when the pH < 8.0.

At very high negative potentials the her takes place dominantly on a metallic zinc surface through the Volmer–Heyrovsky route with the Volmer step being rate controlling, and at a very low surface coverage with H<sub>ads</sub>.

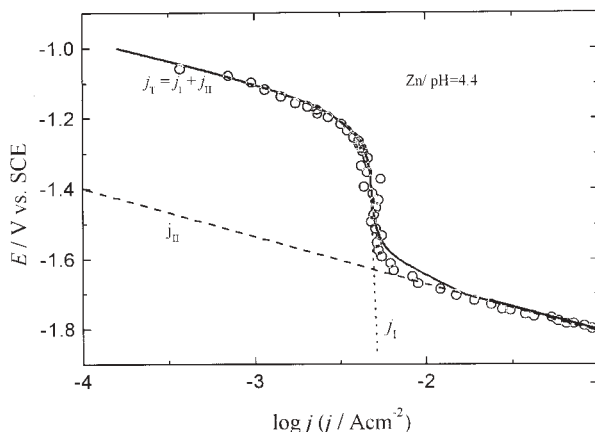


Fig. 7. Potential dependence of the calculated individual rates for the her occurring simultaneously.  $j_I$  – I reaction route,  $j_{II}$  – II reaction route (Volmer–Heyrovsky). The theoretical polarization curve, obtained by summing the individual curve is represented by the full line. The experimental data for the her on Zn in  $1.0 \text{ mol dm}^{-3} \text{ Na}_2\text{SO}_4$  solution (pH 4.4) at  $25.0^\circ\text{C}$  are presented by the circles.

The simulated polarization curve for the first reaction route is presented with a dotted line in Fig. 7. It was obtained using the corresponding values of the rate constants from Table III, the calculated values of the adsorbed intermediates,  $\theta_H$  and  $\theta_O$ , and Eq. (7). The simulated polarization curve for the second reaction route is presented with a dashed line in the same figure. The total current for the her is the sum of two partial currents and is presented as a full line in Fig. 7. It can be seen that the fitted curve is in good agreement with the experimental data, which is an additional support for the correctness of the proposed mechanism of the her.

#### ИЗВОД

#### КИНЕТИКА РЕАКЦИЈЕ ИЗДВАЈАЊА ВОДОНИКА НА ЦИНКУ У СУЛФАТНИМ РАСТВОРИМА

Т. ТРИШОВИЋ<sup>1</sup>, Љ. ГАЛИЋ-КРСТАЈИЋ<sup>1</sup>, Н. КРСТАЈИЋ<sup>2</sup> и М. ВОЈНОВИЋ<sup>2</sup>

<sup>1</sup>Институт за техничке науке - САНУ, Кнеза Михајла 35, Београд и <sup>2</sup>Технолошко-металуршки факултет, Универзитет у Београду, Карнегијева 4, 11000 Београд

Испитивана је кинетика и механизам реакције издвајања водоника (РИВ) на цинку у растворима  $1,0 \text{ mol dm}^{-3} \text{ Na}_2\text{SO}_4$  на  $298 \text{ K}$ , у области рН од 4,4 до 10. Показано је да се применом потенциостатске стационарне волтаметрије и спектроскопије електрохемијске импеданције може одредити механизам ове реакције на цинку. У оквиру испитиване области потенцијала механизам РИВ на цинку се не може објаснити класичним Фолмер-Тафел-Хејровски реакционим путем. Констатовано је да се веома компликован облик катодних поларизационих кривих S-облика, са појавом граничне струје може објаснити одигравањем РИВ преко два паралелна механизма. Први реакциони механизам се састоји од три консекутивна ступња, у којем површински оксид цинка игра активну улогу у РИВ. Други реакциони механизам се састоји од Фолмеровог и Хејровски ступња. Овај механизам РИВ на цинку је доминантан у области негативнијих потенцијала, где се наведена реакција одиграва на металном цинку.

(Примљено 12. јула, ревидирано 29. августа 2001)

## REFERENCES

1. B. N. Kabanov, *Electrochim. Acta* **13** (1968) 19
2. B. N. Kabanov, I. I. Astakhov, I. G. Kiseleva, *Electrochim. Acta* **24** (1979) 167
3. Yu. A. Kukk, V. E. Past, *Elektrokhimiya* **7** (1971) 1863
4. D. C. Walker, *Can. J. Chem.* **45** (1967) 807
5. D. C. Walker, *Q. Rev.* **21** (1967) 79
6. J. C. F. Boodts, S. Trasatti, *J. Appl. Electrochem.* **19** (1989) 255
7. D. M. Dražić, J. Popić, *J. Electroanal. Chem.* **357** (1993) 105
8. M. Elam, B. E. Conway, *J. Appl. Electrochem.* **17** (1987) 1002
9. D. A. Harrington, B. E. Conway, *J. Electroanal. Chem.* **221** (1987) 1
10. B. E. Conway, L. Bai, *J. Chem. Soc., Faraday Trans.* **81** (1985) 1841
11. L. Bai, B. E. Conway, *J. Electrochem. Soc.* **138** (1990) 2897
12. L. Bai, D. A. Harrington, B. E. Conway, *Electrochim. Acta.* **32** (1987) 1713
13. P. Ekolunge, K. Jüttner, G. Kreysa, T. Kessler, M. Ebert, W. J. Lorenz, *J. Electrochem. Soc.* **138** (1991) 2660
14. L. Chen, A. Lasia, *J. Electrochem. Soc.* **138** (1991) 3321
15. E. Potvin, A. Lasia, H. Menard, *J. Electrochem. Soc.* **138** (1991) 900
16. A. Lasia, A. Rami, *J. Electroanal. Chem.* **294** (1990) 123
17. A. K. Cheong, A. Lasia, J. Lessard, *J. Electrochem. Soc.* **140** (1993) 2721
18. D. A. Harrington, B. E. Conway, *Electrochim. Acta* **32** (1987) 11703
19. R. D. Armstrong, M. Henderson, *J. Electroanal. Chem.* **39** (1972) 81
20. Chr. I. Noninski, *Bull. Soc. Chim. France* **9** (1976) 1282
21. L. Gaiser, K. E. Heusler, *Electrochim. Acta* **15** (1970) 161
22. L. Antropov, *Theoretical Electrochemistry*, Mir Publishers Moscow, 1977
23. N. D. Tomashov, L. P. Vershinina, *Electrochim. Acta.* **15** (1970) 502
24. N. D. Tomashov, L. P. Vershinina, N. M. Strukov, *Elektrokhimiya* **5** (1969) 26
25. Chr. I. Noninski, I. P. Ivanov, *Khimiya i industriya* **47** (1975) 70
26. N. V. Krstajić, B. N. Grgur, N. S. Mladenović, M. V. Vojnović, *Electrochim. Acta* **40** (1997) 11703.